4th International Conference on Process Engineering and Advanced Materials

Hydrogen-rich Syngas Production from Ethanol Dry Reforming on La-doped Ni/Al_2O_3 Catalysts: Effect of promoter loading

Mahadi B. Bahari[a], Boon Chin Goo[a], Thong L.M. Pham[b], Tan Ji Siang[a], Huong T. Danh[c], Nurul Ainirazali[a], Dai-Viet N. Vo[a,d,]*

[a]*Faculty of Chemical & Natural Resources Engineering, Universiti Malaysia Pahang,*
Lebuhraya Tun Razak, 26300 Gambang, Kuantan, Pahang, Malaysia
[b]*Institute of Research and Development, Duy Tan University, K7/25 Quang Trung, Da Nang, Vietnam*
[c]*Clean Energy and Chemical Engineering, Korea University of Science and Technology (UST), Daejeon, 305-350, Korea*
[d]*Centre of Excellence for Advanced Research in Fluid Flow, Universiti Malaysia Pahang, 26300 Gambang, Kuantan, Pahang, Malaysia*

Abstract

Ethanol dry reforming has been studied over La-promoted Ni catalysts supported on Al_2O_3 with different promoter loadings at varying CO_2 partial pressure of 20-50 kPa. Catalysts were prepared via co-impregnation technique and characterized using BET surface area, X-ray diffraction measurement, temperature-programmed calcination and scanning electron microscopy. Doped and undoped catalysts possessed high surface area of about 86-108 m^2 g^{-1} and La promoter was well-dispersed on support surface. X-ray diffraction measurements indicated the formation of La_2O_3, NiO and $NiAl_2O_4$ phases in line with temperature-programmed calcination results. La-addition enhanced the dispersion of NiO particles and reduced the agglomeration of metal oxides. Both C_2H_5OH and CO_2 conversions improved with increasing CO_2 partial pressure rationally due to the growing secondary CO_2 reforming of CH_4 reaction. The ratio of H_2/CO produced from ethanol dry reforming varied from 1.1 to 1.4 favored for usage as feedstocks of Fischer-Tropsch synthesis. The yield of H_2 and CO also enhanced with increasing CO_2 partial pressure whilst the optimal La loading in terms of C_2H_5OH conversion was observed at 3%La and catalytic activity increased with promoter addition reasonably owing to the redox properties of La promoter. CO_2 reforming of ethanol reaction appeared via ethanol decomposition to CH_4 intermediate product, which was subsequently converted to CO and H_2 mixture through CH_4 dry reforming reaction.

Keywords: Ethanol dry reforming; Hydrogen; La promoter; Ni-based catalysts; Syngas

* Corresponding author. Tel.: +609 549 2874; fax: +609 549 2889.
E-mail address: vietvo@ump.edu.my (D.-V. N. Vo).

1. Introduction

The persistent and substantial usage of fossil fuels as the main energy has resulted in several urgent concerns including increasing greenhouse gas emissions and the depletion of petroleum-based energy. Syngas referring to the mixture of CO and H_2 has been recognized as a promising alternative energy to reduce the global dependence on crude oil. Currently, steam reforming and partial oxidation of hydrocarbons, namely; methane and propane for syngas generation are the most conventional and economical processes [1, 2]. However, these approaches are unsustainable due to the employment of natural gas, a kind of fossil fuels as feedstocks and emit a large amount of CO_2 gas. Thus, CO_2 reforming of ethanol (cf. Eq. (1)) has gained a significant attention since it not only utilizes a renewable reactant, ethanol which can be derived from highly available biomass [3] but also consumes undesirable CO_2 gas to produce syngas with H_2/CO ratio of around 1 suitable as feedstocks for Fischer-Tropsch synthesis (FTS) [4]. Wang and Wang [5] investigated the thermodynamics of ethanol dry reforming (EDR) using the Gibbs free energy minimization approach and found that high reaction temperature and CO_2-rich reactants enhanced both C_2H_5OH and CO_2 conversions due to reducing carbonaceous deposition.

$$C_2H_5OH + CO_2 \circledR 3H_2 + 3CO \ (\mathrm{VH}_{298K}^0 = 296.8\,\mathrm{kJ\,mol}^{-1}) \tag{1}$$
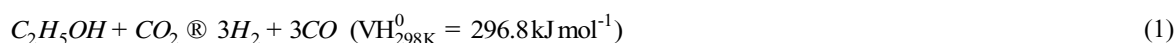
Ni-based catalysts are the common reforming catalyst owing to their inferior cost to precious metals and alleviated C-C bond cleavage [6]. In fact, Zawadzki *et al.* [7] reported that EDR over supported Ni catalyst achieved up to 98% of H_2 yield. However, Ni catalyst was reportedly prone to coke deposition and sintering which deteriorated catalytic activity and stability [7, 8]. Thus, it is crucial to modify Ni catalyst with suitable promoter and supporting materials to keep catalyst surface free of deposited carbon and hence prevent it from deactivation. Lanthanide-group promoters have been used as promoters for CH_4 reforming [9], C_2H_5OH steam reforming [10] and glycerol dry reforming [11] due to their redox properties for carbon gasification. Foo *et al.* [12] found that the addition of lanthanide metal oxides improved the catalytic reactivity and stability of CH_4 dry reforming reaction owing to carbon resilience and increasing basic site concentration.

However, to our best knowledge, the promotional effect of La-dopant on Al_2O_3-supported Ni catalyst for EDR reaction has not been studied. Thus, the objectives of this research were to investigate the physicochemical attributes and performance of La-doped $10\%Ni/Al_2O_3$ catalysts for EDR reaction at different reactant partial pressure. The influence of promoter loading on catalytic activity and selectivity was also examined in this study.

2. Experimental

2.1. Catalyst synthesis

Gamma-alumina support procured from Sigma-Aldrich Chemicals was air-calcined at 973 K for 6 hours to guarantee thermal stability before impregnating with an accurately weighed amount of $Ni(NO_3)_2.6H_2O$ and $La(NO_3)_3.6H_2O$ aqueous solutions. The resulting slurry was then magnetically stirred for 3 hours and dried overnight at 383 K in an oven followed by calcination in air at 873 K for 5 hours with a heating rate of 5 K min^{-1} to synthesize $X\%La-10\%Ni/Al_2O_3$ catalysts (with X: 0-5%).

2.2. Catalyst characterization

The measurement of multi-point BET surface area and pore volume for catalysts was carried out using N_2 physisorption at 77 K in a Thermo Scientific Surfer unit whilst the crystalline structure of γ-Al_2O_3 support and synthesized catalysts was obtained from XRD measurement in Rigaku Miniflex II system. Specimens were scanned from 3-80° with scan speed and step size of 1° min^{-1} and 0.02^0, respectively. Cu target was implemented as radiation source with wavelength, λ of 1.5418 Å and operated at 30 kV and 15 mA. Match! version 3.1.1 software was used for analyzing all X-ray patterns.

In order to investigate the phase formation during calcination in air of impregnated catalyst, temperature-programmed calcination (TPC) was also conducted for uncalcined catalysts on a TGA Q500 unit from TA Instruments. Sample was initially pretreated in N_2 flow of 100 ml min^{-1} for 30 min at 373 K for moisture and volatile compound removal. Specimen was subsequently heated up to 1023 K with a temperature ramping rate of 15 K min^{-1} in 100 ml min^{-1} of $4N_2:O_2$ gas mixture and held isothermally at the same temperature for 30 min before cooling down to ambient temperature in inert gas. The external morphology of catalyst was examined by scanning electron microscope (SEM) measurement in a Carl Zeiss AG - EVO® 50 Series apparatus operated by a SmartSEM software. Acceleration voltage was set in the range of 5 to 16 kV and platinum holder was used for sample analysis.

2.3. Catalyst evaluation

C_2H_5OH dry reforming reaction was conducted in a quartz fixed-bed reactor packed with 0.1 g of catalyst and placed vertically in a split tubular furnace at atmospheric pressure and 973 K. A pair of pressure gauges was mounted at the top and bottom of reactor for continuously monitoring pressure drop through catalyst bed. Gaseous reactant, CO_2 was accurately regulated by an Alicat mass flow controller whilst a KellyMed KL-602 syringe pump was employed for feeding C_2H_5OH into the reactor. CO_2 and C_2H_5OH mixture was diluted in N_2 gas used as a tie component for material balance and ensuring the total flow rate of 70 ml min^{-1}. High gas hourly space velocity, GHSV of 42 L g_{cat}^{-1} h^{-1} and small average particle size of 100-140 μm were employed for each EDR run to guarantee the minimal internal and external transport resistances. The composition of gaseous effluent from the outlet of reactor was determined in an Agilent 6890 Series gas chromatograph (GC) equipped with thermal conductivity (TCD) and flame ionization (FID) detectors.

The catalytic activity and selectivity were assessed in terms of reactant conversion (X_i) and yield (Y_j) of products as given in Eqs. (2)-(6). Additionally, ethanol conversion, X_{C2H5OH} to gaseous products was computed based on the balance of H atoms.

$$X_{C_2H_5OH}\ (\%) = \frac{2F_{H_2}^{Out} + 4F_{CH_4}^{Out}}{6F_{C_2H_5OH}^{In}} \times 100\% \tag{2}$$

$$X_{CO_2}\ (\%) = \frac{F_{CO_2}^{In} - F_{CO_2}^{Out}}{F_{CO_2}^{In}} \times 100\% \tag{3}$$

$$Y_{CH_4}\ (\%) = \frac{F_{CH_4}^{Out}}{F_{CO_2}^{In} + 2F_{C_2H_5OH}^{In}} \times 100\% \tag{4}$$

$$Y_{CO}\ (\%) = \frac{F_{CO}^{Out}}{F_{CO_2}^{In} + 2F_{C_2H_5OH}^{In}} \times 100\% \tag{5}$$

$$Y_{H_2}\ (\%) = \frac{2F_{H_2}^{Out}}{6F_{C_2H_5OH}^{In}} \times 100\% \tag{6}$$

where F^{in} and F^{out} are the inlet and outlet molar flow rates (mol s^{-1}), respectively.

3. Results and Discussion

3.1. Textural properties

The physical properties of calcined γ-Al_2O_3 support, La-promoted and unpromoted 10%Ni/Al_2O_3 catalysts are summarized in Table 1. It is evident that calcined γ-Al_2O_3 support possessed the highest BET surface area of 171.23 m^2 g^{-1} and average pore volume of 0.34 cm^3 g^{-1}. A considerable decline in surface area of about 37% from 171.23 to 108.26 m^2 g^{-1} was observed for 10%Ni/Al_2O_3 catalyst. It was unavoidable due to the presence of NiO particles blocking the porous structure of γ-Al_2O_3 support. The similar decrease in BET surface area was also experienced with the addition of La promoter. However, the mild difference of surface area between 2%La- and 3%La-promoted catalysts would suggest the fine distribution of La dopant on the surface of support.

Table 1. Textural properties of calcined γ-Al_2O_3 support and La-promoted Ni/Al_2O_3 catalyst.

Sample	BET surface area (m^2 g^{-1})	Average pore volume (cm^3 g^{-1})	Average pore diameter (Å)
γ-Al_2O_3	171.23	0.34	52.36
10%Ni/Al_2O_3	108.26	0.28	61.47
2%La-10%Ni/Al_2O_3	98.12	0.28	53.56
3%La-10%Ni/Al_2O_3	86.09	0.22	59.29

3.2. X-ray diffraction measurement

The crystal structure of γ-Al_2O_3 support and La-promoted 10%Ni/Al_2O_3 catalysts was identified by XRD measurements as shown in Fig. 1. All XRD patterns were analysed based on the Joint Committee on Power Diffraction Standards (JCPDS) database [13]. As seen in Fig. 1, the characteristic peaks for γ-Al_2O_3 phase at 2θ of 19.45°, 32.40°, 37.15°, 44.87°, and 68.41° were detected on calcined Al_2O_3 support, La-promoted, and unpromoted 10%Ni/Al_2O_3 catalysts. Regardless of La loading, the diffraction peaks of NiO phase was observed at 2θ = 37.15°, 42.61°, and 62.41° on the surface of both promoted, and unpromoted catalysts. The presence of spinel NiAl$_2$O$_4$ form identified at 2θ of 37.15° and 75.40° was indicative of strong metal-support interaction between NiO particle and γ-Al_2O_3 support. Interestingly, the typical peak at 2θ = 29.87° for La_2O_3 phase was only detected on promoted catalysts with La loading higher than 3% (cf. Figs. 1(d) and (e)). This observation would suggest that at low promoter loading, La_2O_3 phase was well dispersed on support surface and hence was not detectible on X-ray diffractogram.
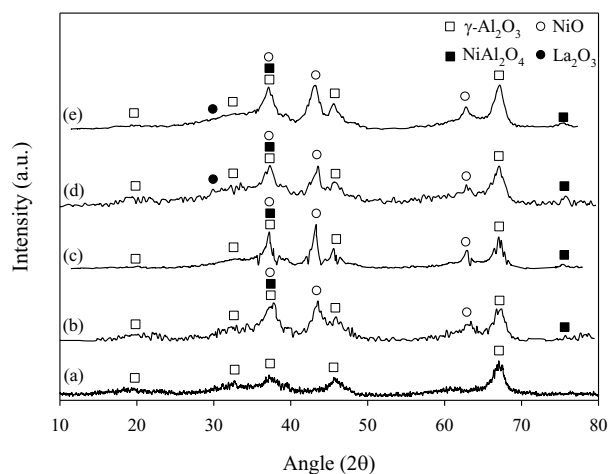

Fig. 1. XRD patterns of (a) calcined γ-Al_2O_3 support, (b) 10%Ni/Al_2O_3, (c) 2%La-10%Ni/Al_2O_3, (d) 3%La-10%Ni/Al_2O_3 and (e) 5%La-10%Ni/Al_2O_3 catalysts.

3.3. Temperature-programmed calcination

The derivative weight profile for temperature-programmed calcination run of a representative La-promoted 10%Ni/Al$_2$O$_3$ catalyst is shown in Fig. 2. The thermal profile has 3 discernible peaks indicating the formation of different metal oxide phases during air-calcination. The low temperature peak with the highest intensity, P1 located at 503 K was ascribed to NiO formation from Ni(NO$_3$)$_2$ decomposition [14] as given in Eq. (7) whilst the second peak, P2 was observed at about 574 K was due to La$_2$O$_3$ production (cf. Eq. (8)).

$$Ni(NO_3)_2 \rightarrow NiO + N_2O_5 \tag{7}$$

$$2La(NO_3)_3 \rightarrow La_2O_3 + 3N_2O_5 \tag{8}$$

The formation of spinel NiAl$_2$O$_3$ phase owing the strong interaction of metal oxides (cf. Eq. (9) was also observed at high temperature of about 800 K (peak P3). As seen in Fig. 2, there were no detectable peaks at temperature greater than 850 K and the derivative weight profile was unchange beyond this temperature indicating that metal precusors were decomposed entirely to the respective metal oxide phases. Since the complete decomposition of these metal nitrates to the corresponding metal oxides played an important role on the degree of catalytic reduction and performance, a high calcination temperature of 873 K was chosen in this study to ensure the optimal production of NiO and La$_2$O$_3$ phases during thermal treatment in flowing air.
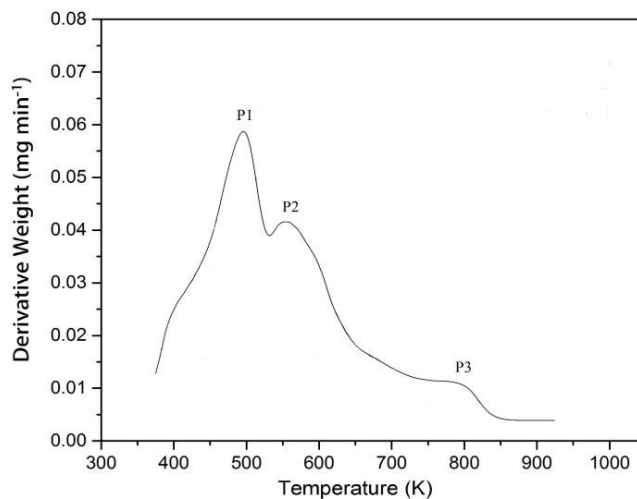
$$NiO + Al_2O_3 \rightarrow NiAl_2O_4 \tag{9}$$

Fig. 2. Derivative weight profile for temperature-programmed calcination of 2%La-10%Ni/Al$_2$O$_3$ catalyst at ramping rate of 15 K min^{-1}.

3.4. SEM analysis

Surface morphology of both promoted and unpromoted catalysts was captured by SEM measurements as seen in Fig. 3. SEM micrograph shows that unpromoted 10%Ni/Al$_2$O$_3$ catalyst possessed a rough surface due to the agglomeration of NiO particles (red circle) on the surface of Al$_2$O$_3$ support (cf. Fig. 3(a)). As seen in Fig. 3(b), it was expected that particle density on the surface of 2%La-10%Ni/Al$_2$O$_3$ catalyst was superior to that of unpromoted counterpart owing to the presence of La$_2$O$_3$ promoter. However, the extent of particle agglomeration seemed to lesser for La-promoted catalyst suggesting that La-dopant would act as a spacer preventing NiO particles from aggregation and hence increasing metal dispersion on catalyst surface.
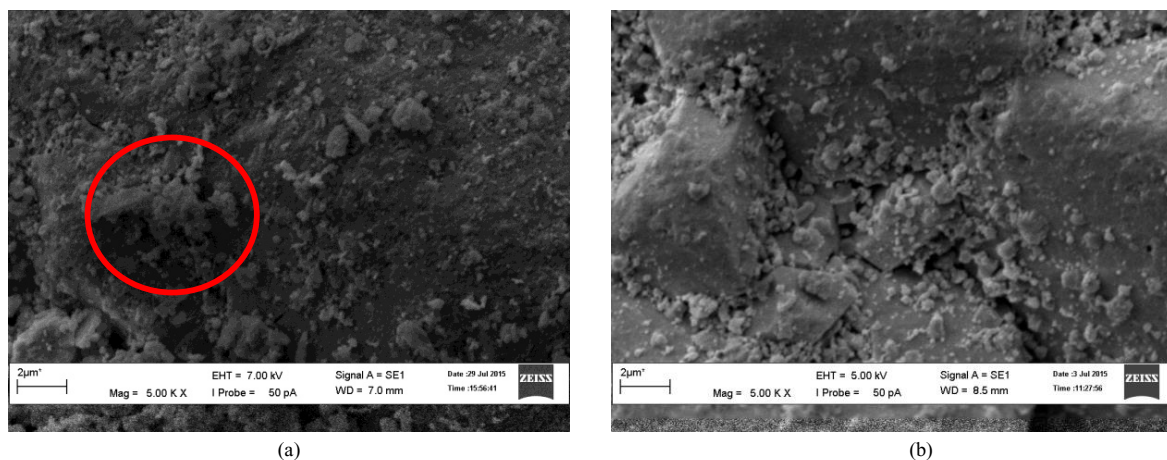
Fig. 3. SEM images of (a) 10%Ni/Al$_2$O$_3$ and (b) 2%La-10%Ni/Al$_2$O$_3$ catalysts.

3.5. Ethanol dry reforming evaluation

3.5.1. Effect of CO$_2$ partial pressure

In order to study the influence of CO$_2$ partial pressure, P$_{CO2}$ on catalytic performance, EDR reaction was conducted over a representative 2%La-10%Ni/Al$_2$O$_3$ catalyst with varying P$_{CO2}$ from 20 to 50 kPa at a constant C$_2$H$_5$OH partial pressure, P$_{C2H5OH}$ of 20 kPa and reaction temperature of 973 K. As seen in Fig. 4(a), C$_2$H$_5$OH and CO$_2$ conversions increased significantly about 38.10% and 52.00%, respectively with growing P$_{CO2}$ from 20-50 kPa reasonably due to the enhancement of CH$_4$ dry reforming reaction, a secondary reaction subsequently converting CH$_4$ intermediate product to syngas. Fig. 4(b) also shows a reduction in CH$_4$/CO ratio about 39.56% with rising P$_{CO2}$ from 20-50 kPa further confirming an increase in CH$_4$ dry reforming rate. In addition, as illustrated in Fig. 5, the yield of CH$_4$ decreased by 34.69% with increasing P$_{CO2}$ whilst an opposite trend was evident for both H$_2$ (129.32%) and CO (88.79%) yields. Irrespective of CO$_2$ partial pressure, the conversion of CO$_2$ (X_{CO2}) was always inferior to C$_2$H$_5$OH conversion (X_{C2H5OH}) as shown in Fig. 4(a). This behaviour indicated the co-existence of simultaneous side reactions including C$_2$H$_5$OH decomposition and dehydrogenation during EDR [7]. Interestingly, the gap between two conversion profiles seemed to be trivially changed with CO$_2$ partial pressure suggesting that the rate of concomitant reactions was not considerably affected by increasing P$_{CO2}$. H$_2$/CO ratio of about 1.1 to 1.4 at P$_{CO2}$ of 20-50 kPa was preferred for downstream FTS [4].
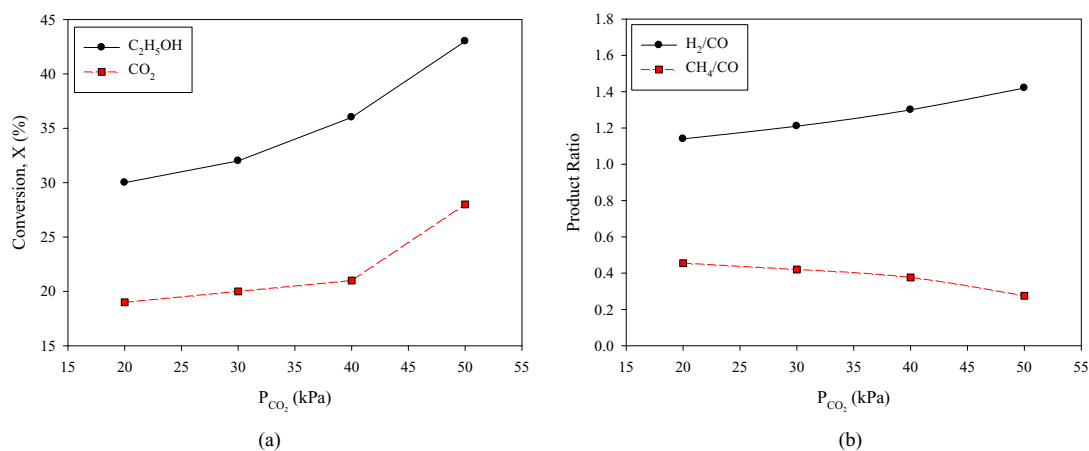

Fig. 4. Effect of P$_{CO2}$ on (a) C$_2$H$_5$OH and CO$_2$ conversions and (b) product ratio at P$_{C2H5OH}$ = 20 kPa and T = 973 K.
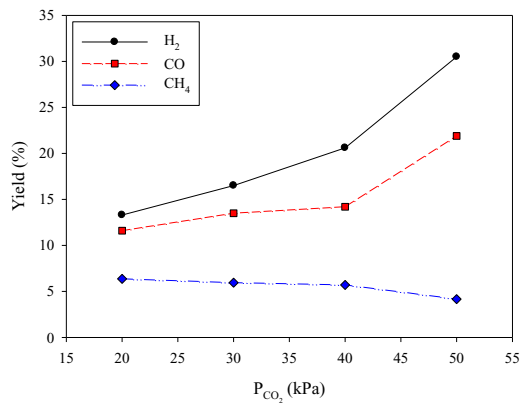
Fig. 5. Effect of P_{CO2} on yield of H_2, CO and CH_4 at P_{C2H5OH} = 20 kPa and T = 973 K.

3.5.2. Effect of La-promoter loading

The influence of promoter loading from 0%La to 5%La on catalytic activity was also examined at P_{C2H5OH} = 20 kPa and 973 K with various P_{CO2} of 20 and 50 kPa. As shown in Fig. 6, La-addition enhanced ethanol conversion and the optimal conversion of C_2H_5OH was observed at 3%La loading for both P_{CO2} of 20 and 50 kPa. The improvement of catalytic activity with the addition of La promoter was reasonably due to the excellent capacity of mobile oxygen storage and release from La dopant [11, 15]. The redox properties of La_2O_3 could gasify the surface carbon to CO_2 and hence protect the active metal surface from carbonaceous deposition [12, 16]. Chen *et al.* found that the in-situ formation of lanthanum dioxycarbonate, $La_2O_2CO_3$ from the reaction between La_2O_3 and CO_2 was resistant to deposited carbon [17]. In addition, the basic property of La promoter reportedly promoted CO_2 adsorption and hence increasing catalytic activity [16, 18]. However, as seen in Fig. 6, a substantial drop in X_{C2H5OH} with La loading beyond the optimum threshold of 3%La rationally due to lesser metal dispersion associated with high metal loading. Interestingly, a reverse relationship between CH_4 yield and La loading was noticed with the minimum CH_4 yield at 2%-3%La loading. This behaviour would suggest that EDR reaction occurred via a 2-step process involving the decomposition of ethanol to methane (cf. Eq. (10)) and the subsequent dry reforming of CH_4 intermediate by-product to syngas mixture (cf. Eq. (11)).
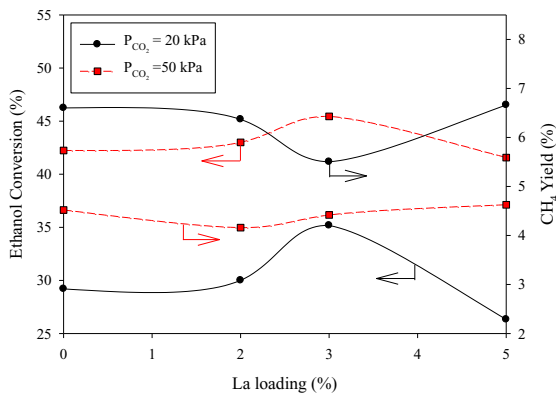
$$C_2H_5OH \circledR CH_4 + CO + H_2 \tag{10}$$

$$CH_4 + CO_2 \circledR 2CO + 2H_2 \tag{11}$$

Fig. 6. Effect of La loading on C_2H_5OH conversion and CH_4 yield at P_{C2H5OH} = 20 kPa and T = 973 K.

4. Conclusion

The promotional effect of La promoter on the physicochemical attributes and catalytic performance of Al_2O_3-supported Ni catalysts for EDR reaction has been investigated at varying P_{CO2} from 20 to 50 kPa and a constant P_{CH4} of 20 kPa. La-addition prevented NiO particles from aggregating on support surface. Thus, both promoted and unpromoted catalysts exhibited high BET surface area of 86-108 m^2 g^{-1}. The conversions of C_2H_5OH and CO_2 increased considerably about 38.10% and 52.00% in that order with an increase in P_{CO2} from 20-50 kPa most likely due to the growing CH_4 dry reforming reaction. Interestingly, the resulting H_2/CO ratio ranging from 1.1. to 1.4 was suitable for downstream FTS to produce long-chain hydrocarbons. The yield of CH_4 experienced a linear decline with the growth of P_{CO2} whilst a reverse trend was evident for H_2 and CO yields suggesting that CH_4 dry reforming reaction was an important secondary reaction, which subsequently converted CH_4 by-product formed from ethanol decomposition to H_2 and CO. Ethanol conversion increased with La loading and approached an optimal value at 3%La loading because of the high mobile oxygen storage capacity of La_2O_3 oxidizing carbonaceous deposition on catalyst surface and preventing catalyst from deactivation.

Acknowledgements

References

[1] V. Arcotumapathy, D.-V. N. Vo, D. Chesterfield, C.T. Tin, A. Siahvashi, F.P. Lucien, A.A. Adesina, Catalyst design for methane steam reforming, Appl. Catal. A: Gen. 479 (2014) 87-102.
[2] G. Karoshi, P. Kolar, S.B. Shah, G. Gilleskie, L. Das, Calcined eggshell as an inexpensive catalyst for partial oxidation of methane, J. Taiwan Inst. Chem. Eng. 57 (2015) 123-128.
[3] M.S. Batista, R.K.S. Santos, E.M. Assaf, J.M. Assaf, E.A. Ticianelli, High efficiency steam reforming of ethanol by cobalt-based catalysts, J. Power Sources. 134 (2004) 27-32.
[4] D.-V.N. Vo, V. Arcotumapathy, B. Abdullah, A.A. Adesina, Non-linear ASF product distribution over alkaline-earth promoted molybdenum carbide catalysts for hydrocarbon synthesis, Catal. Today 214 (2013) 42-49.
[5] W. Wang, Y. Wang, Dry reforming of ethanol for hydrogen production: Thermodynamic investigation, Int. J. Hydrogen Energy 34 (2009) 5382-5389.
[6] M. Li, X. Wang, S. Li, S. Wang, X. Ma, Hydrogen production from ethanol steam reforming over nickel based catalyst derived from Ni/Mg/Al hydrotalcite-like compounds, Int. J. Hydrogen Energy 35 (2010) 6699-6708.
[7] A. Zawadzki, J.D.A. Bellido, A.F. Lucredio, E. M. Assaf, Dry reforming of ethanol over supported Ni catalysts prepared by impregnation with methanolic solution, Fuel Process. Technol. 128 (2014) 432-440.
[8] X. Hu, G. Lu, Syngas production by CO_2 reforming of ethanol over Ni/Al_2O_3 catalyst, Catal. Commun. 10 (2009) 1633-1637.
[9] H. Ay, D. Üner, Dry reforming of methane over CeO_2 supported Ni, Co and Ni–Co catalysts, Appl. Catal. B: Environ. 179 (2015) 128-138
[10] P. Osorio-Vargas, N.A. Flores-González, R.M. Navarro, J.L.G. Fierro, C.H. Campos, P. Reyes, Improved stability of Ni/Al_2O_3 catalysts by effect of promoters (La2O3, CeO2) for ethanol steam-reforming reaction, Catal. Today 259 (2016) 27-38.
[11] K.W. Siew, H.C. Lee, J. Gimbun, S.Y. Chin, M.R. Khan, Y.H. Taufiq-Yap, C.K. Cheng, Syngas production from glycerol-dry (CO2) reforming over La-promoted Ni/Al2O3 catalyst, Renew. Energy 74 (2015) 441-447.
[12] S.Y. Foo, C.K. Cheng, T.-H. Nguyen, A.A. Adesina, Evaluation of lanthanide-group promoters on Co–Ni/Al2O3 catalysts for CH4 dry reforming, J. Mol. Catal. A: Chem. 344 (2011) 28-36.
[13] JCPDS Powder Diffraction File, International Centre for Diffraction Data, warthmore, PA, 2000.
[14] K. Selvarajah, N.H.H. Phuc, B. Abdullah, F. Alenazey, D.-V.N. Vo, Syngas production from methane dry reforming over Ni/Al2O3 catalyst, Res. Chem. Intermed. DOI 10.1007/s11164-015-2395-5.
[15] D. Li, L. Zeng, X. Li, X. Wang, H. Ma, S. Assabumrungrat, J. Gong, Ceria-promoted Ni/SBA-15 catalyst for ethanol steam reforming with enhanced activity and resistance to deactivation, Appl. Catal. B: Environ. 176-177 (2015) 532-541.
[16] U. Oemar, Y. Kathiraser, L. Mo, X.K. Ho, S. Kawi, CO2 reforming of methane over highly active La-promoted Ni supported on SBA-15 catalysts: mechanism and kinetic modelling, Catal. Sci. Technol. DOI: 10.1039/C5CY00906E.
[17] H. Chen, H. Yu, F. Peng, H. Wang, J. Yang, M. Pan, Efficient and stable oxidative steam reforming of ethanol for hydrogen production: effect of in situ dispersion of Ir over Ir/La2O3, J. Catal. 269 (2010) 281-290.
[18] L. Qian, Z. Ma, Y. Ren, H. Shi, B. Yue, S. Feng, J. Shen, S. Xie, Investigation of La promotion mechanism on Ni/SBA-15 catalysts in CH4 reforming with CO_2, Fuel 122 (2014) 47-53.